Equivalent Field Calculation to Irregular Symmetric and Asymmetric Photon Fields

N. Chegeni and M. J. Tahmasebi Birgani

Abstract—Equivalent fields are frequently used for central axis depth-dose calculations of rectangular and irregular shaped photon beam. Since most of the proposed models to calculate the equivalent square field, are dosimetry-based, a simple physical-based method to calculate the equivalent square field size was used as the basis of this study. The table of the sides of the equivalent square for rectangular fields was constructed and then compared with the well-known tables of BJR and Venselaar with the average relative error percentage of 2.5±2.5 % and 1.5±1.5 % respectively. To evaluate the accuracy of this method, the PDDs were measured for some special irregular symmetric and asymmetric treatment fields and their equivalent squares for Siemens Primus Plus linear accelerator for both energies 6 and 18MV. The mean relative differences of PDDs measurement for these fields and their equivalent square was approximately 1% or less. As a result, this method can be employed to calculate equivalent field not only for rectangular fields but also for any irregular symmetric or asymmetric field.

Keywords—Equivalent field, asymmetric field, irregular field, multi leaf collimators.

I. INTRODUCTION

NOWADAYS, equivalent fields are frequently used, mostly as equivalent squares both in regular and in irregular field photon-beam dose calculations for radiotherapy [2]. Although the convolution/superposition algorithms have reduced the need for using this technique in some aspects of treatment planning, it is widely used in monitor unit (MU) checks with manual or automated dose calculation programs for the purpose of having a double check system on the outcome of the complex TPS calculation and to speed up calculation in irregular fields of photon beams as well as to reduce measurement time [3], [4]. The equivalent fields are defined as the fields of standard shape (circular or square) which have the same central-axis depth-dose characteristics as the given field [5], but was later applied to other field size dependent parameters, such as scatter factors and output factors [6].

The square to circular field equivalence can be done by using the conversion method, which was previously described by Day and Aird and discussed, in more detail, by Bjärngard

N. Chegeni is with the Department of Radiation Therapy, Golestan Hospital, JondiShapour University of Medical Science, Ahvaz, Iran (phone: 98916-353-4022; e-mail: nchegen@yahoo.com).
M. J. Tahmasebi Birgani is with the Department of Medical Physics, JondiShapour University of Medical Sciences, Ahvaz, Iran (e-mail: tahmasebi_mj@yahoo.com).
The authors would like to thank the office of Vice-Chancellor for Research of JoundiShapour University of Medical Science Ahvaz, Iran.

and Siddon [7]:

$$2R_{eq}/S = 1.123 - 0.00067S \qquad (1)$$

where R_{eq} is the radius of the equivalent circular, and S the side of the square field, both defined at the surface (i.e. at SSD=100cm). The equivalent field to the rectangular fields tabulated in the British Journal of Radiology supplement 25 [6] is based on Clarkson's method [8] which used a model for scatter-radius function by data fitting. The usage of the equivalent square from BJR-table can just be recommended for prediction of output factor, with the shorter side of the field set by upper jaws and longer side by lower jaws [9]. A simple approximate method to calculate the collimator scatter factor proposed by sterling [10] is based on the assumption that the dose for rectangular field can be equated to that of the square field if their area to perimeter (A/P) are the same which has been improved by the elongation correction factor [7]-[11] and for a blocked field [12].

The new energy-specific table was constructed by averaging 4 energy-specific tables for ^{60}Co, 6, 10, and 25 MV photon beams and using a three-Gaussian model which could eventually lead to a difference of 0.5 - 1.0% in the value of phantom scatter (S_P), compared to the use of the BJR-table [1]. Sanz et al., [13] also presented an analytical calculation of dose errors arising when field equivalencies calculated at certain reference depth, are transferred to the other depths.

In the most studies mentioned above, the models are based on data fitting using measurements; therefore, electron disequilibrium leads to an underestimate for small fields [14]. Furthermore, for irregular asymmetric fields used in Intensity-modulated radiation therapy, one has to employ complicated Clarkson's method or the method proposed by Day [15], [16]. In this research, we put forth an analytical method for field equivalency and show it is capable to calculate equivalent field for any irregular asymmetric field. Then calculation results will be compared for some routine treatment fields with dosimetry measurements.

II. THEORETICAL BACKGROUND

A. Calculation of Equivalent Field

For any fixed point at fixed depth on the central axis in the medium, the primary component of the dose will be the same for all fields. It therefore follows which equivalency between standard and nonstandard fields is determined by the requirement that the contribution to the dose along the central

axis from scattered photons for the two fields be equal [6]. Consider a reference plane normal to the central axis, placed at the fixed source-to-surface distance (e.g. 100cm). The field bound generated by the collimators can be projected over this plane as X1, X2, Y1 and Y2. The origin is on the central axis. Suppose that there is a parallel beam striking the surface of the phantom. Hence, each element (dx.dy) on the surface acts as a source of scattered radiation. The amount of scatter radiation reaching to the central axis is inversely proportional to the square of the distance between surface elements and the origin; therefore, an asymmetric irregular field (e.g., an asymmetric field with some shielded parts by Cerrobend blocks or multi-leaf collimators (MLC)) to circular field equivalence at the central axis is calculated using the following equation (Fig. 1 (a)):

$$\int_{X2}^{X1}\int_{Y2}^{Y1}\frac{dxdy}{x^2+y^2}-(1-e^{-\mu t})\iint_{shielded\ parts}\frac{dxdy}{x^2+y^2}=\iint_{equivalent\ circle}\frac{dxdy}{x^2+y^2} \quad (2)$$

where μ (cm^{-1}) and t (cm) are the attenuation coefficient and thickness of the blocks or the leaves of MLC respectively. The second part of the left side of (1) shows the share of the total scatter from all shielded parts.

1. Symmetric Fields

Suppose that the contribution of scattered radiation reaching the central axis of a rectangular field with dimensions W×Lcm^2 (Fig. 1 (a)) and a circular field of radius R_{eq} (cm) on a plane at SSD=100cm (Fig. 1 (c)) is considered to be equal. Equation (2) can be simplified as follows:

$$\int_{-W/2}^{W/2}\int_{-L/2}^{L/2}\frac{dxdy}{x^2+y^2}=\iint_{equivalent\ circle}\frac{dxdy}{x^2+y^2} \quad (3)$$

Let us eliminate the small area at the origin of coordinate with radius ε (refers to ion chamber radius) to overcome of singularity and use polar system (Fig. 1 (b)). Equation (3) will be modified as (4).
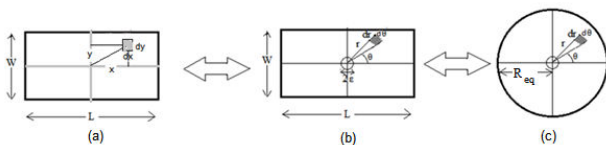

Fig. 1 The rectangular field with dimension W×L cm2 (in Cartesian coordinates (a) and in polar coordinates (b)) is equivalent to a circular field with radius R_{eq} cm (c) on a plane at SSD=100cm

$$\int_{0}^{\tan^{-1}(\frac{W}{L})}\int_{\varepsilon\to0}^{\frac{L}{2\cos\theta}}\frac{drd\theta}{r}+\int_{\tan^{-1}(\frac{W}{L})}^{\frac{\pi}{2}}\int_{\varepsilon\to0}^{\frac{W}{2\sin\theta}}\frac{drd\theta}{r}=\int_{0}^{\pi/2}\int_{\varepsilon\to0}^{R_{eq}}\frac{drd\theta}{r} \quad (4)$$

where ε is expected to be eliminated because it is presented on both sides of (4). After integrating from both sides of (4) with some mathematic operations, it can be rewritten as:

$$2R_{eq}=W\left(\frac{L}{W}\right)^{\frac{2}{\pi}\tan^{-1}(\frac{W}{L})}\exp\left(-\frac{2}{\pi}\int_{\tan^{-1}(\frac{W}{L})-\frac{\pi}{2}}^{\tan^{-1}(\frac{W}{L})}\ln(\cos\theta)d\theta\right) \quad (5)$$

As a special case, the circular field equivalent to a square field is obtained by substituting S (side of square) rather than W and L in (5).

$$2R_{eq}=S\exp\left(-\frac{2}{\pi}\int_{-\pi/4}^{\pi/4}\ln(\cos(\theta))d\theta\right) \quad (6)$$

By applying the numerical calculation software (MATLAB), (6) would simplify to:

$$2R_{eq}/S=1.116 \quad (7)$$

As a result, the square field equivalent to a rectangular field can be obtained by replacing 1.116 S_{eq} instead of $2R_{eq}$ in (6).

$$S_{eq}=\frac{W}{1.116}\left(\frac{L}{W}\right)^{\frac{2}{\pi}\tan^{-1}(\frac{W}{L})}\exp\left(-\frac{2}{\pi}\int_{\tan^{-1}(\frac{W}{L})-\frac{\pi}{2}}^{\tan^{-1}(\frac{W}{L})}\ln(\cos\theta)d\theta\right) \quad (8)$$

2. Asymmetric Fields

Modern linear accelerators are equipped with collimators that allow independent setting of each jaw. The application of asymmetrically collimated beams has become increasingly common in many clinical standard situations. In the case of asymmetric jaw positions, the center of the field is off the central axis of the collimator. So for a square to asymmetric field equivalency, the asymmetric field has to be divided into four parts [17]. The following equation is therefore extracted,

$$S_{eq}=\frac{2\sqrt{Y1Y2}}{1.116}\left(\frac{X1}{Y1}\right)^{\frac{\tan^{-1}(\frac{Y1}{X1})}{2\pi}}\left(\frac{X1}{Y2}\right)^{\frac{\tan^{-1}(\frac{Y2}{X1})}{2\pi}}\left(\frac{X2}{Y1}\right)^{\frac{\tan^{-1}(\frac{Y1}{X2})}{2\pi}}\left(\frac{X2}{Y2}\right)^{\frac{\tan^{-1}(\frac{Y2}{X2})}{2\pi}}\times$$
$$\exp\left(\frac{-1}{2\pi}\left(\begin{array}{c}\int_{\tan^{-1}(Y1/X1)-\pi/2}^{\tan^{-1}(Y1/X1)}\ln(\cos\theta)d\theta+\int_{\tan^{-1}(Y2/X1)-\pi/2}^{\tan^{-1}(Y2/X1)}\ln(\cos\theta)d\theta+\\ \int_{\tan^{-1}(Y1/X2)-\pi/2}^{\tan^{-1}(Y1/X2)}\ln(\cos\theta)d\theta+\int_{\tan^{-1}(Y2/X2)-\pi/2}^{\tan^{-1}(Y2/X2)}\ln(\cos\theta)d\theta\end{array}\right)\right) \quad (9)$$

where Y1, Y2, X1, X2 are collimator apertures at the phantom surface.

3. Irregular Fields

Shaping the beam is an important way of minimizing the absorbed dose in healthy tissue and critical structures. Conventional collimator jaws are used for shaping a rectangular treatment field (Y1, Y2, X1, X2); however, as the treatment volume is not usually rectangular, additional shaping is required. On a linear accelerator, lead or Cerrobend blocks are attached on to the treatment head under standard collimating system. MLC as a further alternative has movable leaves, which can block some fractions of the radiation beam. Therefore, when a portion of the radiation field has to be covered to protect healthy tissue, to calculate the equivalent

square field, the scattering contribution from the shielded parts should be subtracted (Fig. 2). For this purpose, (9) is changed by subtracting the share of the total scatter from all shielded parts, as (10):

$$S_{eq} = \frac{2\sqrt{Y1\,Y2}}{1.116}\left(\frac{X1}{Y1}\right)^{\frac{\tan^{-1}(\frac{Y1}{X1})}{2\pi}}\left(\frac{X1}{Y2}\right)^{\frac{\tan^{-1}(\frac{Y2}{X1})}{2\pi}}\left(\frac{X2}{Y1}\right)^{\frac{\tan^{-1}(\frac{Y1}{X2})}{2\pi}}\left(\frac{X2}{Y2}\right)^{\frac{\tan^{-1}(\frac{Y2}{X2})}{2\pi}} \times$$

$$\exp\left[\frac{-1}{2\pi}\left(\begin{array}{c}\int_{\tan^{-1}(\frac{Y1}{X1})-\frac{\pi}{2}}^{\tan^{-1}(\frac{Y1}{X1})}\ln(\cos\theta)d\theta + \int_{\tan^{-1}(\frac{Y2}{X1})-\frac{\pi}{2}}^{\tan^{-1}(\frac{Y1}{X1})}\ln(\cos\theta)d\theta + \int_{\tan^{-1}(\frac{Y1}{X2})-\frac{\pi}{2}}^{\tan^{-1}(\frac{Y1}{X2})}\ln(\cos\theta)d\theta + \\ \int_{\tan^{-1}(\frac{Y2}{X2})-\frac{\pi}{2}}^{\tan^{-1}(\frac{Y2}{X2})}\ln(\cos\theta)d\theta - (1-e^{-\mu t})\sum_{i=1}^{n}\iint_{shield\ i^{th}}\frac{dxdy}{x^2+y^2}\end{array}\right)\right]$$

(10)

where n shows the number of blocks or leaves. As can be seen in Fig. 2, to calculate scatter contribution under the blocked parts, one can write:
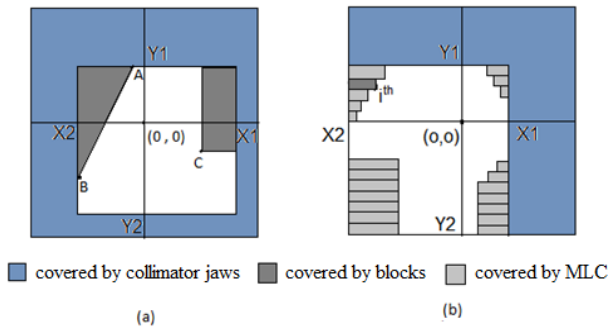

Fig. 2 An asymmetric field with shielded parts by Cerrobend blocks (a) and MLC (b)

$$\sum_{shielded\ parts}\iint\frac{dxdy}{x^2+y^2} =$$

$$\begin{cases}\int_{X2}^{x_A}\int_{y(x)}^{Y1}\frac{dxdy}{x^2+y^2} + \int_{x_C}^{X1}\int_{y_C}^{Y1}\frac{dxdy}{x^2+y^2} & \text{(blocks)} \\ \sum_{left\ leaves}\int_{y_i}^{y_i+l}\int_{X2}^{x_i}\frac{dxdy}{x^2+y^2} + \sum_{right\ leaves}\int_{y_i}^{y_i+l}\int_{x_i}^{X1}\frac{dxdy}{x^2+y^2} & \text{(MLC)}\end{cases}$$

(11)

where all coordinates $(x_A, x_C,\ldots)$ are defined at the surface (i.e. at SSD) and the leaf width is lcm at the surface of the phantom and $y(x)$ is equation of the line AB as follows:

$$y(x) = \left(\frac{y_A - y_B}{x_A - x_B}\right)x + \left(\frac{x_A y_B - x_B y_A}{x_A - x_B}\right)$$

(12)

III. MATERIAL AND METHOD

The linear accelerator used in this study was Siemens Primus Plus which can deliver x-rays of nominal energies 6 and 18 MV operated at a dose rate of 300 MU/min. The treatment unit was equipped with independent jaws assigned to as Y1 and Y2 for the upper and X1 and X2 for the lower jaws at SSD=100cm. A Scanditronix blue phantom

(Wellhofer, Germany) (50 cm ×50 cm ×50 cm) with two 0.13cm3 ionization chambers (IBA, CC13, Germany) were employed for the measurements. Omni-Accept pro6.5 software (Wellhofer, Germany) was utilized for collecting and recording data from two chambers.

The phantom scatter related quantity to assess the accuracy of the equivalent field method in this study was percentage depth dose (PDD). To validate this method, PDD for some symmetric, asymmetric, irregular, and wedged photon fields (as shown in Fig. 3-7) and their calculated equivalent squares were measured along the central axis. All field sizes were defined at 100 cm from the source according to the fixed source surface distance (SSD=100) and formed by the secondary collimators system and Cerrobend blocks for shielding.

A general computer program using MATLAB 7.12.0 software was written to calculate the equivalent square side for any open or wedged field (symmetric, asymmetric, and asymmetric wedged fields) and shielded field (shielded symmetric, shielded asymmetric).

IV. RESULTS AND DISCUSSION

The most general method for irregular or asymmetric field dose calculation is based on separation of the radiation into primary and scatter component [8], [13], [18]. The primary component of the radiation for any shaped field is the same, and only differences in the scatter component affect dose quantity. In this study, to calculate the scatter contribution from all parts of the radiation field to the central axis, the amount of scatter radiation reaching to the central axis was considered inversely proportional to the square of the distance between all points of the irradiated field and the central axis. As can be seen, for the square to circular field equivalency, (7) shows approximately an agreement with that shown in (1) by Day and Aird [6].

Tables of equivalent square fields are applied to reduce the number of dose measurements required by the increasing possibilities of treatment machines (e. g., being equipped with asymmetric jaws or MLC); therefore, according to (8), the equivalent squares were obtained for a series of rectangular fields which demonstrated in Table I.

TABLE I
EQUIVALENT SQUARES FOR RECTANGULAR FIELDS WITH DIMENSIONS FROM 2 CM TO 40 CM CALCULATED BY (8)

Side of the Field (cm)	4.0	6.0	8.0	10.0	12.0	14.0	16.0	18.0	20.0	30.0	40.0
4.0	4.0										
6.0	4.8	6.0									
8.0	5.3	6.8	8.0								
10.0	5.6	7.4	8.9	10.0							
12.0	5.8	7.9	9.5	10.9	12.0						
14.0	6.0	8.2	10.1	11.6	12.9	14.0					
16.0	6.1	8.5	10.5	12.2	13.7	14.9	16.0				
18.0	6.2	8.7	10.9	12.7	14.3	15.7	16.9	18.0			
20.0	6.3	8.9	11.2	13.1	14.9	16.4	17.7	18.9	20.0		
30.0	6.6	9.5	12.1	14.5	16.7	18.8	20.6	22.3	23.9	30.0	
40.0	6.7	9.8	12.6	15.3	17.8	20.1	22.3	24.4	26.3	34.2	40.0

Comparing the results in Table I with BJR-table and the tables provided by Venselaar [1] were made using $\%Diff_{with\,x} = 100 \times (S_{eq,x} - S_{eq,Eq.9})/S_{eq,x}$; where x indicates BJR or Venselaar (they were not shown here). The comparison for rectangular fields where one dimension is 4cm or greater revealed the findings of this study are closer to the table provided by Venselaar with maximum 0.8 cm and mean difference (%Diff) of 1.5±1.5 %. As well as the differences between Table I and BJR-table is at maximum 1.8 cm and the average percentage of 2.5±2.5%. However, as can be seen from Table II, the findings of current study for the rectangular fields where one dimension is equal to 2cm do not support the previous studies showing the mean %Diff with BJR and Venselaar's 13.8±3.7% and 15.2±2.5% respectively. These differences can be explained in part by the lack of lateral electronic equilibrium for small fields. In other words, the standard method for calculating equivalent squares leads to an underestimate of S_P for fields in which one dimension is too small to permit lateral electronic equilibrium; therefore Thomas et al., [14] presented a new formula for the equivalent square, specifically for use in calculating S_p values. It had a similar form to Vadash's formula [11], except the smaller and larger field dimensions (Xmin and Xmax) are used, and in place of the empirical constant A an empirical variable B is used:

$$S_{eq} = (B+1)X_{min}X_{max} / (BX_{min} + X_{max}) \quad (13)$$

where B=B(Xmin) is itself a function of the smaller field dimension. For a Siemens Oncor, they obtained B=0.52 + 0.45 ln (Xmin). In this method, the electronic disequilibrium issue exists on both sides of (2) for small fields; therefore, this effect will be disappeared.

We calculated the equivalent square for some small fields using (13) as shown in the fifth column of Table II. The results indicate the mean %Diff equal to 0.4±0.9 (see Table II the last column). However, due to the approximation method proposed by Thomas for small fields, further evaluation is necessary.

In order to assess the accuracy of the equivalent field method in this research for shielded and asymmetric fields, the calculation is done by first finding the equivalent square by solving (10) for some special treatment fields (shown in Fig. 3-7). Afterward, PDDs were measured on the central axis of those fields and their equivalent fields which have been plotted. To calculate relative differences between PDD measured for every field (F) and its equivalent square (S_{eq}) at depth d, $RE\% = \left| \dfrac{PDD_{measured}(d,F) - PDD_{measured}(d,S_{eq})}{PDD_{measured}(d,F)} \right| \times 100$ was used.

Fig. 3, 4 represents the PDD measured for shielded symmetric field applied in pelvic and gastric cancer treatment. The average RE% for 6 and 18 MV were 0.5±0.4% and 0.4±0.7% respectively for pelvic treatment and 0.5±0.6% and 0.5±1.1% respectively for gastric treatment.

For asymmetric fields, Fig. 5 shows asymmetric field 10×10 with 3cm offset and its equivalent square field 8×8with the average RE% was 0.6±0.9%. PDD for an asymmetric shielded field (10×20 with 5cm offset) was measured (Fig. 6). The RE% was 0.5±0.6% for 6MV.
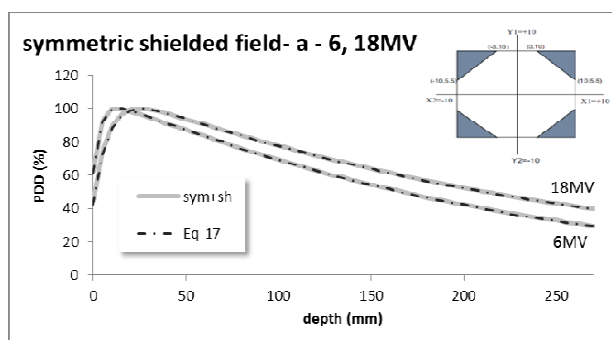

Fig. 3 The PDD measured for a shielded symmetric field 20×20 applied for pelvic cancer as showed in the graph (gray line) and its calculated equivalent square 17×17 (dash-dot) for 6 & 18MV energies with relative error 0.5±0.4% and 0.4±0.7%, respectively

TABLE II
EQUIVALENT SQUARE FIELD SIDE (SEQ) OF RECTANGULAR FIELDS CALCULATED USING EQ.8 HAVE BEEN COMPARED WITH THOSE FROM BJR, VENSELAAR'S FINDINGS [1] AND THOMAS'S METHOD [14] (13) FIELDS WHICH ONE DIMENSION IS EQUAL TO 2CM USING WHERE X INDICATES BJR, VENSELAAR AND THOMAS

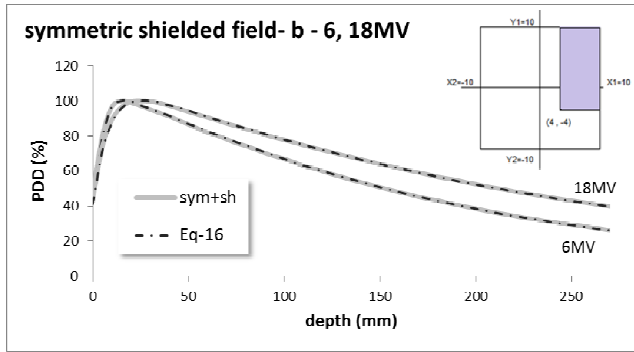| Fields (cm²)	Eq. 8 (cm)	BJR (cm)	Venselaar (cm)	Thomas (cm)*	%Diff with BJR	%Diff with Venselaar	%Diff with Thomas
2×4	2.6	2.7	2.8	2.6	2.7	6.2	-1.6
2×6	2.9	3.1	3.3	2.9	6.3	12.0	-1.3
2×8	3.1	3.4	3.6	3.0	10.0	15.0	-0.9
2×10	3.2	3.6	3.7	3.1	12.3	14.7	-0.5
2×12	3.2	3.7	3.8	3.2	12.9	15.2	-0.2
2×16	3.3	3.9	4.0	3.3	15.1	17.3	0.3
2×20	3.4	4.0	4.0	3.4	15.9	15.9	0.6
2×22	3.4	4.0	4.0	3.4	15.5	15.5	0.7
2×26	3.4	4.1	4.1	3.4	16.8	16.8	0.9
2×30	3.4	4.1	4.1	3.5	16.2	16.2	1.1
2×32	3.4	4.1	4.1	3.5	16.0	16.0	1.1
2×36	3.5	4.1	4.1	3.5	15.6	15.6	1.2
2×40	3.5	4.1	4.1	3.5	15.3	15.3	1.3

using Eq.13 where B=0.52+0.45 ln(Xmin).

Fig. 4 The PDD measured for a shielded symmetric field 20×20 applied for gastric cancer as showed in the graph (gray line) and its calculated equivalent square 16×16 (dash-dot) for 6 & 18MV energies with relative error 0.5±0.6% and 0.5±1.1%, respectively
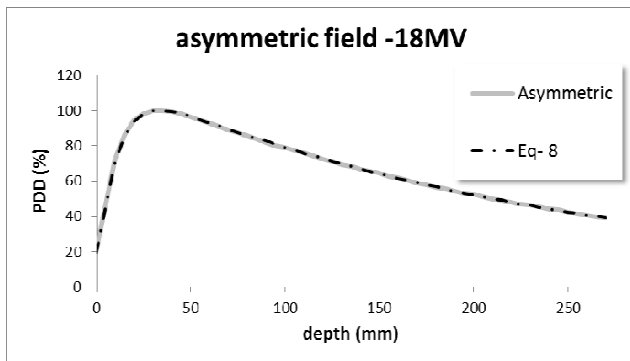

Fig. 5 The PDD measured for an asymmetric rectangular field (5, 5×2, 8) (gray line) and its calculated equivalent square 8×8 (dash-dot) for 18MV energies with relative error 0.6±0.9%
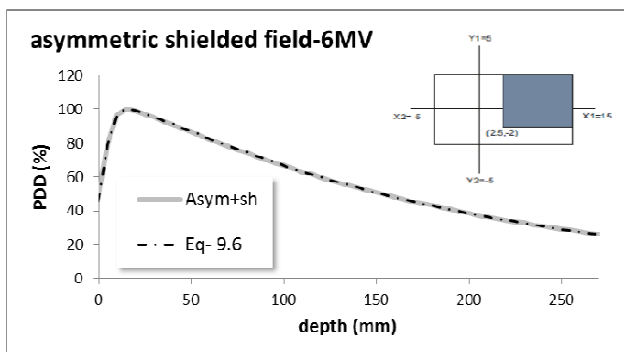

Fig. 6 The PDD measured for a shielded asymmetric field (5, 5 x 5, 15) as showed in the graph (gray line) and its calculated equivalent square 9.6×9.6 (dash-dot) for 6 MV energies with relative error 0.09±0.10%

For most photon beam qualities, no change on S_P has been observed if a wedge is inserted in a photon beam [19]. However, it can result in a different PDD curve compared to the open beam due to beam hardening or softening especially for high energy photon beams. Therefore, after equivalent field calculation for wedged field, the wedge was inserted to

measure PDD for both asymmetric wedged field (10×10 with 3cm offset) and its equivalent field 8×8 (dash-dot) (Fig. 7). The average RE% for 6 and 18 MV was 0.9±1.51% and 0.64±1.3% respectively.
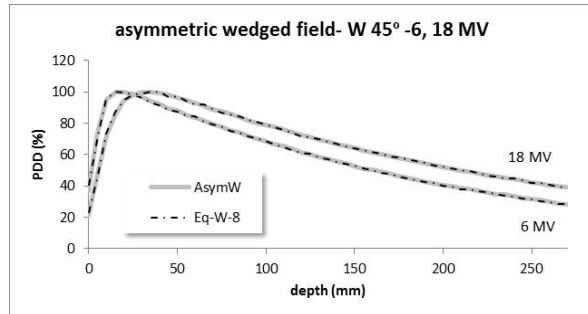

Fig. 7 The PDD measured for an asymmetric wedged field (5, 5×2, 8) (gray line) for 45º wedge and its calculated equivalent square 8×8 (dash-dot) for 6 & 18MV energies with relative error 0.9±1.51% and 0.64±1.3%, respectively

V. CONCLUSIONS

Most mathematical models proposed with respect to the concept of the equivalent square in the previous literature, involved some constant or variable coefficients were determined using a myriad of measurements and fittings. And also, these models lead to an underestimate for small fields in which one dimension is too small to permit lateral electronic equilibrium [14]. In this study, we have applied a simple physical-based model and showed that it is in agreement with previous studies for rectangular fields. As well as, it can be applied for any irregular asymmetric field. Moreover, (2) can be rewritten for any point (x_0, y_0) off-axis by replacing $(x - x_0)^2 + (y - y_0)^2$ left in the denominators. Furthermore, this method may be useful for the more complex MLC geometries treatment fields that are nowadays used more often than in earlier times using (10), (11). Finally, this method can be implemented in clinic mostly for hand calculation.

APPENDIX

In this appendix, the procedure to transition (5) from (4) is explained. Integration with respect to r leads to natural logarithm as follows:

$$\int_0^{\tan^{-1}(W/L)} \ln(\frac{L}{2\varepsilon \cos\theta})\,d\theta + \int_{\tan^{-1}(W/L)}^{\pi/2} \ln(\frac{W}{2\varepsilon \sin\theta})\,d\theta = \int_0^{\pi/2} \ln(\frac{R_{eq}}{\varepsilon})\,d\theta \quad \text{(A-1)}$$

In the next step, integration respect to θ, the following equation is obtained.

$$\tan^{-1}(\frac{W}{L}).\ln(\frac{L}{W}) + \frac{\pi}{2}\ln(\frac{W}{2\varepsilon}) - \int_0^{\tan^{-1}(W/L)} \ln(\cos\theta)\,d\theta - \int_{\tan^{-1}(W/L)}^{\pi/2} \ln(\sin\theta)\,d\theta = \frac{\pi}{2}\ln(\frac{R_{eq}}{\varepsilon}) \quad \text{(A-2)}$$

and also

$$R_{eq} = \frac{W}{2}\left(\frac{L}{W}\right)^{\frac{2}{\pi}\tan^{-1}(W/L)} \exp\left(-\frac{2}{\pi}\left(\int_0^{\tan^{-1}(W/L)} \ln(\cos\theta)\,d\theta + \int_{\tan^{-1}(W/L)}^{\pi/2} \ln(\sin\theta)\,d\theta\right)\right) \quad \text{(A-3)}$$

Finally by more simplification, it will be rearranged as (5).

REFERENCES

[1] Venselaar, J.L., et al., Is there a need for a revised table of equivalent square fields for the determination of phantom scatter correction factors? Phys Med Biol, 1997. 42(12): p. 2369-81.

[2] Yu Jin, H., et al., A simplified method for the calculation of equivalent squares of irregular photon fields. ConfProc IEEE Eng Med BiolSoc, 2005. 7: p. 7091-4.

[3] McCurdy, B.M. and S. Pistorius, Determination of equivalent photon fields through integrated 1D convolution kernels. Phys Med Biol, 1999. 44(12): p. 2971-85.

[4] Storchi, P. and E. Woudstra, Calculation of the absorbed dose distribution due to irregularly shaped photon beams using pencil beam kernels derived from basic beam data. Phys Med Biol, 1996. 41(4): p. 637-56.

[5] Day, M.J., A note on the calculation of dose in x-ray fields. British Journal of Radiology 1950. 23(270): p. 368-9.

[6] Day, M.J. and E.G. Aird, The equivalent field method for dose determinations in rectangular fields. British Journal of Radiology Suppl, 1996. 25: p. 138-51.

[7] Bjärngard, B.E. and R.L. Siddon, A note on equivalent circles, squares, and rectangles. Med Phys, 1982. 9(2): p. 258-60.

[8] Clarkson, J.R., A note on depth doses in fields of irregular shape. British Journal of Radiology, 1941. 14: p. 265- 268.

[9] Sathiyan, S., M. Ravikumar, and S.L. Keshava, Relative Output Factors and Absolute Equivalent Square Fields at Depths for High Energy X-Ray and Gamma Ray Beams. Austral Asian Journal of Cancer 2006. 5(4): p. 225-235.

[10] Sterling, T., H. Perry, and J. Weinkam, Automation of radiation treatment planning. VI. A general field equation to calculate percent depth dose in the irradiated volume of a cobalt 60 beam. British Journal of Radiology, 1967. 40(474): p. 463-74.

[11] Vadash, P. and B. Bjärngard, An equivalent-square formula for head-scatter factors. Med Phys, 1993. 20(3): p. 733-4.

[12] Monti, A.F., et al., An equivalent square method for irregular photon fields. Med Dosim, 1995. 20(4): p. 275-7.

[13] Sanz, D.E., Accuracy limits of the equivalent field method for irregular photon fields. Phys Med Biol, 2002. 47(17): p. 3073-85.

[14] Thomas, S.J., et al., Equivalent squares for small field dosimetry. Br J Radiol, 2008. 81(971): p. 897-901.

[15] Araki, F., et al., Dose calculation for asymmetric photon fields with independent jaws and multileaf collimators. Med Phys, 2000. 27(2): p. 340-5.

[16] Kwa, W., et al., Dosimetry for asymmetric x-ray fields. Med Phys, 1994. 21(10): p. 1599-604.

[17] Day, M.J., The equivalent field method for axial dose determinations in rectangular fields. British Journal of Radiology, 1972. 11: p. Suppl 11:95-10.

[18] Stathakis, S., et al., An inhomogeneity correction algorithm for irregular fields of high-energy photon beams based on Clarkson integration and the 3D beam subtraction method. J ApplClin Med Phys, 2006. 7(1): p. 1-13.

[19] Heukelom, S., J.H. Lanson, and B.J. Mijnheer, Wedge factor constituents of high-energy photon beams: head and phantom scatter dose components. RadiotherOncol, 1994. 32(1): p. 73-83.